ELSEVIER

Polymer 44 (2003) 1711–1719

polymer

www.elsevier.com/locate/polymer

Surface morphology and Flory–Huggins interaction strength in UCST blend system comprising poly(4-methyl styrene) and isotactic polystyrene

L.L. Chang, E.M. Woo*

Department of Chemical Engineering, National Cheng Kung University, Tainan 701-01, Taiwan, ROC

Received 9 September 2002; received in revised form 29 October 2002; accepted 22 November 2002

Abstract

The surface morphology and polymer–polymer interaction parameter (χ_{12}) of UCST blend systems comprising isotactic polystyrene and poly(4-methyl styrene) (P4MS) were investigated using atomic-force microscopy (AFM) and differential scanning calorimetry (DSC). From the measured glass transition temperature and the specific heat increments (ΔC_p) at T_g, it was found that the P4MS dissolved more easily in the iPS rich-phase than did the iPS in the P4MS rich-phase. AFM result also supported that the compatibility increased more in the regions of P4MS-rich compositions than in the regions of PS-rich compositions of the PS/P4MS blends. From the measured T_g's and apparent weight fractions of iPS and P4MS dissolved in each phase, the values of the Flory–Huggins interaction parameter (χ_{12}) were determined to be 0.0163–0.0232 depending on the composition. These results indicate that the χ_{12} is quite dependend on the apparent volume fraction of the polymers dissolved in each phase. The values of χ_{12} calculated from this work (method based on T_g's of phases) were lower than those estimated using an earlier method based on the UCST or clarity temperatures. All values of χ_{12} are greater than the values of interaction parameter at the critical point $(\chi_{12})_c$. This fact indicates that the iPS/P4MS blend are immiscible for all blend compositions. The surface of the phase-separated blend system was mostly covered with the P4MS rich-phase owing to its lower surface free energy in comparison with that of the neat iPS. The mechanism of surface phase separation for the P4MS blends with aPS or iPS is governed by two factors: (1) difference in the solubility of the two polymers in the solvent and (2) surface free energy.

Keywords: Poly(4-methyl styrene); Isotactic polystyrene; UCST

1. Introduction

An earlier study in our laboratory has led to discovery of miscibility in the blend of poly(cyclohexyl methacrylate) with poly(4-methyl styrene) (P4MS) [1]. Other than a few literature-documented examples, styrenic polymers are mostly immiscible with each other polymers. Thus, miscibility in blends involving styrenic polymers is relatively rare and of a great interest. The upper-critical-solution-temperature (UCST) behavior in blends of atactic polystyrene (aPS) and isotactic polystyrene (iPS) with P4MS has been earlier reported and modeled [2–7]. Blend systems that are immiscible (phase-separated) at ambient temperature but can become miscible upon heating to high temperatures with a UCST are relatively rare. Most polymer mixtures are immiscible at ambient and remain immiscible regardless temperature changes. One of our earlier studies [7] has led to a conclusion of miscibility in the blend of iPS with P4MS. It is known to be immiscible and exhibits two glass transition temperatures designated as $T_{g(iPS)}$ for the iPS-rich phase, and $T_{g(P4MS)}$ for the P4MS-rich phase. The T_g's of the iPS-rich phase decrease almost linearly with an increase in the weight fraction of iPS for the iPS/P4MS blends. The above phenomenon also can be seen in this study of the morphology of the iPS/P4MS blends later.

For immiscible polymer blends, the need to know the polymer–polymer interaction parameter (χ_{12}) arises because of its influence on the morphology of the domain structure and the thickness of the transition layer between the domains. The degree of miscibility of polymer blends can provide important information for designing desired structure-property balances and is usually understood in terms of the Forry–Huggins interaction parameter (χ_{12}) between the component polymers. Many methods are available for evaluation of the interaction parameter for

* Corresponding author. Tel.: +886-6275-7575x62670; fax: +886-6234-4496.
E-mail address: emwoo@mail.ncku.edu.tw (E.M. Woo).

0032-3861/03/$ - see front matter © 2003 Elsevier Science Ltd. All rights reserved.
PII: S0032-3861(02)00915-1

miscible blends [8–14]. The most practical among them is the one relying on the determination of binodal and spinodal temperatures as a function of the composition. The binodal curve can be determined by the light scattering method as described by Scholte [15] or a refined method as developed by Gordon et al. [16]. A few methods have been developed to determine the χ_{12} value for phase-separated polymer blend systems, and most are ternary-solution methods [17,18]. Differential scanning calorimetry (DSC) may be the most convenient method to determine the χ_{12} value of phase-separated polymer blends in the solid state. This technique has been widely used for polystyrene (PS)/polycarbonate (PC) [19], PC/poly(methyl methacrylate) (PMMA) [20], PS/PMMA [21], and PC/poly(ethylene terephthalate) (PET) [22] by Burns et al. The χ_{12} value can be calculated using DSC data from the experimental value of the glass transition temperature (T_g) and heat capacity increment (ΔC_p).

Surface morphology is an important subject of studies for polymer blends. Immiscible blends generally exhibit segregated structures with domains predominantly from the individual homopolymers. It is shown that changing the relative homopolymer proportions in such blends leads to variations in the domain structure and surface morphology [23]. Both grains and holes morphologies have been observed depending on the blend compositions and film thickness [24,25]. Another important aspect of immiscible blends is the tendency for one of the homopolymers to be enriched at the surface in preference to the other. The phenomenon of surface enrichment has been reported for the blend systems of PC/PMMA [26–28], poly(sebacic anhydride) (PSA)/poly(lactic acid) (PLA) [29], PS/PMMA [23,24,30–33]. In PC/PMMA blends [26–28], the surface segregation of PMMA has always been observed even when PC nodules are present in the bulk. For the PSA/PLA blends [29], the surfaces are enriched with PLA component at all compositions. Kajiyama et al. [24,25,31], and Bradley et al. [23,30] have investigated the phase-separated structure of the immiscible PS/PMMA blend films by using atomic force microscopy (AFM) for understanding the mechanism of phase separation. Both PS and PMMA-rich phases are observed at surface. The surface covered with PS segments with lower surface free energy is thermodynamically stable state. The driving forces for surface enrichment can be caused by differences in the surface free energies of the polymer components [34,35]. In general, the component with a lower surface free energy is enriched at the surface in order to minimize the surface tension. Although the surface enrichment in polymer blends has been widely studied, surface segregation [36,37] in blends with specific interactions has received little attention.

Earlier study has mainly focused on blends of isotactic PS with P4MS showing an interesting UCST behavior [7]. Scanning electron microscopy (SEM) characterization has revealed the details of phase domains in the blend system, and a phase-in-phase morphology is apparent in which the iPS component is distributed as a continuous phase enclosing discrete and relatively large P4MS-rich domain of a spherical shape. However, none of the previous studies have investigated on effects of interaction parameter on the trends of variation of the phase morphology. The objectives of this study were to examine the polymer–polymer interaction parameter (χ_{12}) and surface morphology in immiscible iPS/P4MS blend system by using experimentally determined glass transition temperature and AFM, respectively. With the aid of powerful resolution of AFM, focus in this study was placed on understanding the effects of interaction parameter on the phase-separated structure of the iPS/P4MS blend system.

2. Experimental

2.1. Materials and sample preparation

Isotactic polystyrene (iPS, with 90% isotacticity) was purchased from Scientific Polymer Products, Inc., with $M_w = 400{,}000$ g/mol (Gel Permeation Chromatograph, GPC), and a T_g of 95 °C. P4MS, also called poly(*p*-methyl styrene), was obtained from Scientific Polymer Products (SP^2), Inc. (USA), with an approximate $M_w = 100{,}000$ g/mol (GPC) with a polydispersity index (PI) of about 3.3 and $T_g = 106–110$ °C (onset). The polymer materials were free of additives and were used without further purification. The characteristics of iPS and P4MS used in this study are summarized in Table 1.

The blend samples in this study were prepared by solvent-casting at slightly above ambient temperature (45 °C), and tetrahydrofuran (THF) was used for preparation of all blend samples. All solution-cast blend samples were subjected to vacuum degassing at a final temperature of 80–90 °C for two days to ensure complete removal of residual solvent.

2.2. Apparatus

2.2.1. Differential scanning calorimeter (DSC)

The glass transition temperatures were measured with a DSC (Perkin–Elmer DSC-7) equipped with an intracooler and a computer for data acquisition/analysis. To ensure obtained accurate results, temperature calibration was

Table 1
Characterization of iPS and P4MS used in this study

	$\bar{M}_w$[a]	T_g[b] (°C)	ΔC_p[b] (J/g K)	γ[c] (mJ/m^2)	δ[c] (MPa$^{1/2}$)
iPS[d]	400,000	89.14	0.30	40.7	18.60
P4MS[d]	100,000	106.5	0.31	38.7	19.33

[a] Measured in scientific polymer products by GPC (THF, 25 °C).
[b] Measured in our laboratory by DSC.
[c] Obtain from Ref. [56].
[d] Supplied by scientific polymer products (SP^2).

performed using zinc ($T_m = 419.47$ °C) and indium ($T_m = 156.6$ °C) as standards. All T_g measurements were made at a scan rate of 20 °C/min, and the T_g values were taken as the onset of the transition in the DSC traces.

2.2.2. Atomic force microscopy (AFM)

AFM measurements were performed at ambient conditions with a scanning probe microscope MultiMode NanoScope (Digital Instruments, Santa Barbara, CA, USA). A standard MultiMode SPM was equipped with an optical detection head, scanner and microscope base. Experiments were conducted in tapping mode with commercial silicon cantilever probes. In comparison to contact-mode operation, the tapping mode is known to minimize the sample distortion due to mechanical interactions between the AFM tip and surface. Commercial silicon probes, each with a normal tip radius of 5–10 nm and spring constant in the range of 20–100 N/m (values provided by manufacturer) were oscillated at their resonance frequencies, which ranged between 250–300 kHz. The largest scan area was $12.4 \times 12.4\ \mu m^2$. Images were recorded with the highest sampling resolution, i.e. 512×512 data points.

3. Results and discussion

3.1. Estimation of phase compositions of iPS/P4MS blends

Two T_g's were detected in the phase-separated iPS/P4MS blends [7], therefore, two phases containing different fractions of these two polymer components were apparent. Since the iPS/P4MS blend was composed of two phases, with one being the iPS-rich phase and the other being the P4MS-rich phase, the phase compositions in these two phases could then be estimated using several methods based on the measure T_g's. Burns and Kim [38–41] have used two T_g's data to investigate the phase compositions of immiscible polymer blends. From the T_g's of iPS and P4MS, we can estimate the apparent weight fractions of iPS and P4MS dissolved in the iPS-rich phase and the P4MS-rich phase, respectively. Estimations of the compositions of these two phases were attempted. The procedures are illustrated as follows. The Wood equation is given [42]:

$$T_g = w_1 T_{g1} + w_2 T_{g2} \tag{1}$$

where T_g is the glass transition temperature of the blend, and w_i and T_{gi} are the weight fraction and the T_g of polymer i (1 or 2). T_{g1} is designated as that for the component possessing the lower T_g. Eq. (1) can be rearranged as [43]:

$$\omega_1' = (T_{g1,b} - T_{g2})/(T_{g1} - T_{g2}) \tag{2}$$

where ω_1' is the apparent weight fraction of iPS in iPS-rich phase, $T_{g1,b}$ is the observed T_g of the iPS-rich phase in the blends, and T_{g1}, T_{g2} are the T_g's of homopolymer 1 and 2, respectively. Similarly, Eq. (1) can also be rearranged to:

$$\omega_1'' = (T_{g2,b} - T_{g2})/(T_{g1} - T_{g2}) \tag{3}$$

where ω_1'' is the apparent weight fraction of iPS in P4MS-rich phase, and $T_{g2,b}$ is the observed T_g of the P4MS-rich phase in the iPS/P4MS blend. The apparent weight fractions of iPS and P4MS components in the phases can also be determined by using the Fox equation [44] and the Couchman equation [45,46], which are used to predict T_g's for miscible polymer blends. The Fox equation [44] is given by

$$1/T_g = w_1/T_{g1} + w_2/T_{g2} \tag{4}$$

where w_1 and w_2 represent the weight fraction of the component, and T_g, T_{g1} and T_{g2} are the T_g's of the blend, component 1 and 2, respectively. Eq. (4) can be rearranged as:

$$\omega_1' = T_{g1}(T_{g1,b} - T_{g2})/[T_{g1,b}(T_{g1} - T_{g2})] \tag{5}$$

where ω_1' is the apparent weight fraction of iPS in iPS-rich phase, $T_{g1,b}$ is the observed T_g of the iPS-rich phase. The Couchman equation [45,46] predicts the values of T_g and ΔC_p at T_g for miscible polymer blends and is given by:

$$\ln T_g = (w_1 \Delta C_{p1} \ln T_{g1} + w_2 \Delta C_{p2} \ln T_{g2})/(w_1 \Delta C_{p1} + w_2 \Delta C_{p2}) \tag{6}$$

where $\Delta C_p = C_p^l(T_g) - C_p^s(T_g)$ = difference in the molar heat capacity at T_g, and $\Delta C_p^l(T_g)$ and $\Delta C_p^s(T_g)$ are the specific heat capacity of the liquid state and solid state, respectively. Eq. (6) can also be rearranged as:

$$\omega_1' = [\Delta C_{p2}(\ln T_{g1,b} - \ln T_{g2})]/[\Delta C_{p1}(\ln T_{g1} - \ln T_{g1,b}) + \Delta C_{p2}(\ln T_{g1,b} - \ln T_{g2})] \tag{7}$$

By substituting Eqs. (2), (5) and (7) to the T_g model for the iPS/P4MS blends, the apparent weight fraction of iPS in the iPS-rich phase (ω_1') and in the P4MS-rich phase (ω_1'') were calculated. Fig. 1 shows the phase diagrams based on the apparent weight fraction (ω_1' and ω_1'') and overall weight

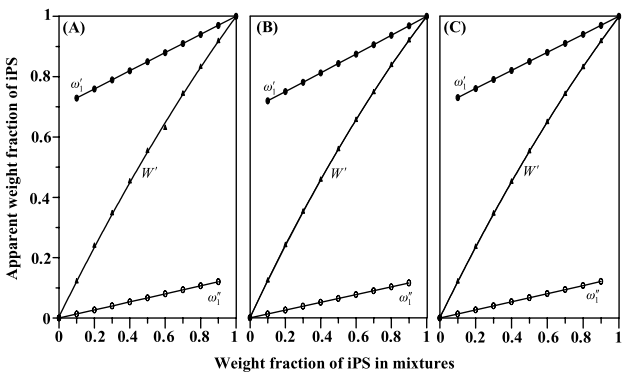

Fig. 1. Comparison of apparent weight fraction (ω) and overall weight fraction (W) of iPS and P4MS components in the iPS-rich phase and P4MS-rich phase by using (A) Wood; (B) Fox; and (C) Couchman relations.

fraction (W' and W'') of iPS and P4MS components in the iPS-rich phase and P4MS-rich phase of iPS/P4MS blends by using (A) Wood, (B) Fox, and (C) Couchman relations. It shows that the amount of P4MS dissolved in the iPS-rich phase (ω_2') is greater than the amount of iPS dissolved in the P4MS-rich phase (ω_1''). The overall weight fractions of the iPS-rich phase (W') and P4MS-rich phase (W''), respectively, in the blends can be calculated by the following expressions [38]:

$$W_{1T} = \omega_1' W' + \omega_1'' W'' \tag{8}$$

$$W_{2T} = \omega_2' W' + \omega_2'' W'' \tag{9}$$

where W_{1T} and W_{2T} are the overall weight fractions of iPS and P4MS in blends, respectively. The values of ω_1' and ω_1'' could be obtained from the previously equations, respectively. Lower W' values (iPS-rich phase) and higher W'' values (P4MS-rich phase) with increasing P4MS concentrations in the blend were observed.

3.1.1. Specific heat increment (ΔC_p) of iPS/P4MS

The values of ΔC_p for the iPS-rich phase and P4MS-rich phase in iPS/P4MS blends prepared by solution casting are shown in Fig. 2, which were calculated from the T_g data [7]. The ΔC_p at the T_g of the iPS-rich phase decreases with an increase in the weight fraction of P4MS. Apparently, decrease of $\Delta C_{p(iPS)}$ with the weight fraction of iPS is more significant than decrease of $\Delta C_{p(P4MS)}$ with the weight fraction of P4MS. Two explanations have been proposed for interpreting the decrease of specific heat increment (ΔC_p) at T_g [47]. One explanation is that the size of the dispersed phase is very small so that the magnitude of the specific heat increment (ΔC_p) of each phase decreases. The other explanation is that both iPS and P4MS phases diffuse into an interfacial region. Many studies [38–41,48–50] have concluded that the reduction in the ΔC_p of each component to the dissolution of that component in the conjugate phase. The result indicates that some of the iPS component is dissolved in the P4MS-rich phase and some of the P4MS is dissolved in the iPS-rich phase.

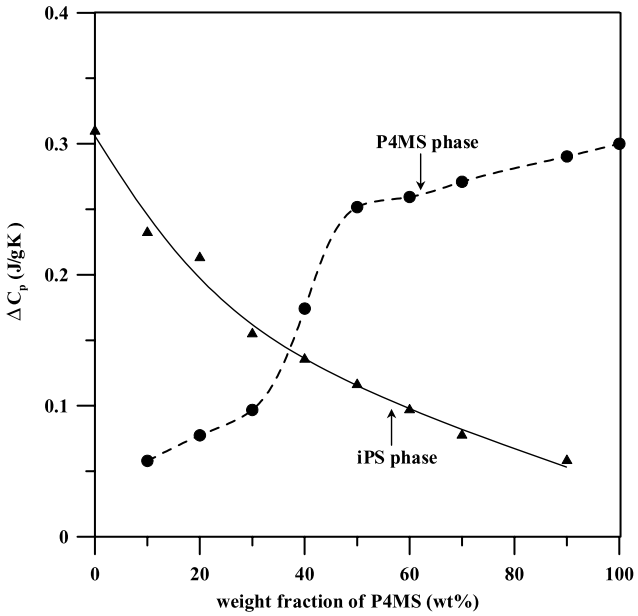

Fig. 2. Specific heat increment (ΔC_p) at T_g for iPS (▲) and P4MS (●) in iPS/P4MS blends.

3.1.2. Polymer–polymer interaction parameter

In application of the thermodynamic criteria to the study of phase equilibrium in polymeric systems, the Gibbs free energy of mixing, ΔG_m, for a system consisting of two polymers from the Flory–Huggins theory can be written as follows [51–53]:

$$\Delta G_m = RT[n_1 \ln \phi_1 + n_2 \ln \phi_2 + \chi_{12}\phi_1\phi_2(m_1 n_1 + m_2 n_2)] \tag{10}$$

where ΔG_m is the free energy of mixing per mole of lattice site, ϕ_1 and ϕ_2 are the volume fractions of the polymers. The χ_{12} is the Flory–Huggins interaction parameter and n_i is the number of moles of the ith component in the mixture. The m_i is the degree of polymerization, relating the molar volumes V_1 and V_2 of the polymers to a fictitious molar volume V_0 of one submolecule of polymer.

Burns and Kim have used the DSC technique to determine the χ value for some phase-separated polymer blends from the T_g data [19–22,38–41]. The phase compositions are shown in Table 2. The χ_{12} equation can be derived as a function of phase compositions [19–22, 38–41] with the consideration of size difference between the repeating unit of the compositions. Thus, the Flory–Huggins polymer–polymer interaction parameter (χ_{12}) of the blends can be determined by using Eq. (11) [38–41]:

$$\chi_{12} = \frac{\{(\phi_1'^2 - \phi_1''^2)[m_2 \ln(\phi_1''/\phi_1') + (m_1 - m_2)(\phi_2' - \phi_2'')] + (\phi_2'^2 - \phi_2''^2)[m_1 \ln(\phi_2''/\phi_2') + (m_2 - m_1)(\phi_1' - \phi_1'')]\}}{2m_1 m_2(\phi_1'^2 - \phi_1''^2)(\phi_2'^2 - \phi_2''^2)} \tag{11}$$

where ϕ_1' is the apparent volume fraction of iPS in the iPS-rich phase, ϕ_1'' is the apparent volume fraction of iPS in the P4MS-rich phase, and m_1, m_2 are the degree of polymerization of iPS and P4MS components, respectively.

The Flory–Huggins polymer–polymer interaction parameter (χ_{12}) could be caculated by using Eq. (11). The volume fraction was obtained from weight fraction divided by densities of each polymer. It shows that the values of χ_{12} are compared for three different ways of the treatment of apparent weight fraction of iPS and P4MS components by the Wood, Fox, and Couchman relations. The values of χ_{12} were found to be 0.0163–0.0232 for the solution-cast blends

Table 2
Comparison of polymer–polymer interaction parameter (χ_{12}) by the Wood, Fox, and Couchman equations

iPS (wt%)	T_{g1} (°C)	T_{g2} (°C)	Wood equation, χ_{12}[a]	Fox equation, χ_{12}[a]	Couchman equation, χ_{12}[a]
0		106.5			
10	93.8	106.2	0.0163	0.0163	0.0163
20	93.3	106.0	0.0158	0.0158	0.0158
30	92.8	105.8	0.0158	0.0157	0.0158
40	92.3	105.5	0.0160	0.0159	0.0161
50	91.8	105.3	0.0165	0.0164	0.0165
60	91.2	105.1	0.0172	0.0171	0.0172
70	90.7	104.9	0.0183	0.0182	0.0183
80	90.2	104.6	0.0200	0.0198	0.0200
90	89.7	104.4	0.0231	0.0229	0.0232
100	89.1				

[a] All χ_{12} were calculated from Eq. (11).

at 45 °C, and are in good agreement among the three different ways of estimating the weight fractions of components in the phases. The interaction parameter at the critical point $(\chi_{12})_c$ can be derived easily from the degree of polymerization and the repeating unit volume of the components. This value can serve as a criterion for predicting the phase stability or phase separation of a blend if the value of $(\chi_{12})_c$ is determined. The $(\chi_{12})_c$ can be calculated by using Eq. (12) [54]:

$$(\chi_{12})_c = \frac{1}{2}(m_1^{-1/2} + m_2^{-1/2})^2 \quad (12)$$

Using Eq. (12), the value of $(\chi_{12})_c$ was found to be 0.01175 for iPS/P4MS blends. It can be surmised that if $\chi_{12} < (\chi_{12})_c$ then the polymers are miscible with each other (no phase separation). On the other hand, if $\chi_{12} > (\chi_{12})_c$ in the blends, phase separation can occur [55]. The values of χ_{12} are greater than the values of $(\chi_{12})_c$, thus the iPS/P4MS blends are immiscible for all blend compositions.

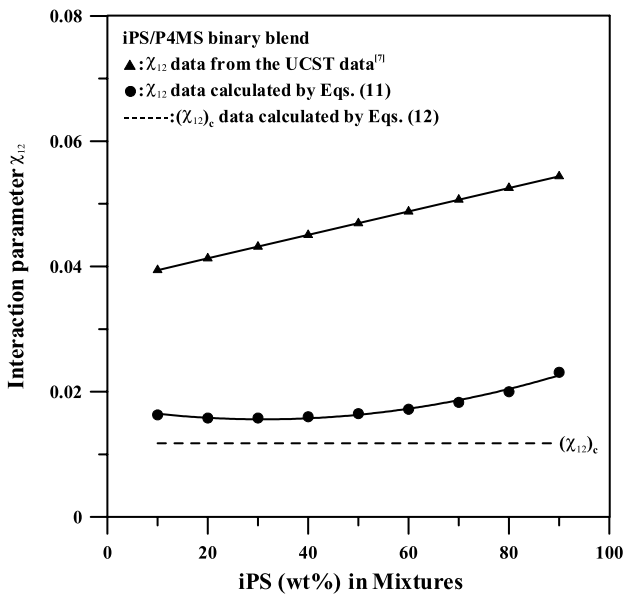

Fig. 3. The values of χ_{12} for the iPS/P4MS blends calculated by a modified Flory–Huggins expression using the experimental UCST data and the T_g results. The values of $(\chi_{12})_c$ were calculated form Eq. (12).

Fig. 3 shows the relation between χ_{12} and weight fraction obtained by the Eqs. (11) and (12). It also shows the values of χ_{12} for the iPS/P4MS blends calculated by a modified Flory–Huggins expression using the experimental UCST data, as discussed in one of our earlier studies [7]. The χ_{12} values obtained from the UCST data are slightly larger than those found in this study for iPS/P4MS blends from the T_g results. All values of χ_{12} are greater than those of $(\chi_{12})_c$. This fact indicates that the iPS/P4MS blends are immiscible for all blend compositions. It is interesting to note that the interaction parameter (χ_{12}) increases with the weight fraction of iPS in the blends. It appears that the compatibility increases more in the region of P4MS-rich compositions than in the region of iPS-rich compositions in the iPS/P4MS blends. It should be mentioned here that the method of the UCST data as discussed in the earlier report [7] could only be employed in blend systems that exhibit a UCST behavior. Therefore, the method based on T_g's of the separated phases can be a more practical way to measure χ_{12}, especially for general blend systems that exhibit partially misciblility or completely phase-separation.

3.1.3. Estimation surface morphology by AFM

The samples of neat iPS, P4MS, and the blends containing different compositions of the polymers displayed distinctly different surface morphologies when analyzed with AFM. Figs. 4 and 5 show (A) AFM image, (B) sectional view along the line in the AFM image, and (C) the three-dimensional topography for pure iPS and P4MS, respectively. The AFM image shows an irregular surface structure with apparent height of about 1000 nm for the neat iPS, and the neat P4MS shows an uneven surface with a maxim height of about 100 nm. The neat iPS displays a quite different fracture surface morphology and much more irregular surface patterns than pure P4MS. Therefore, this result indicates that solvent (THF) was more quickly removed from P4MS segment than iPS, and thus the iPS segment tended to stay longer in the liquid phase due to a higher solubility of the iPS in the solvent of THF

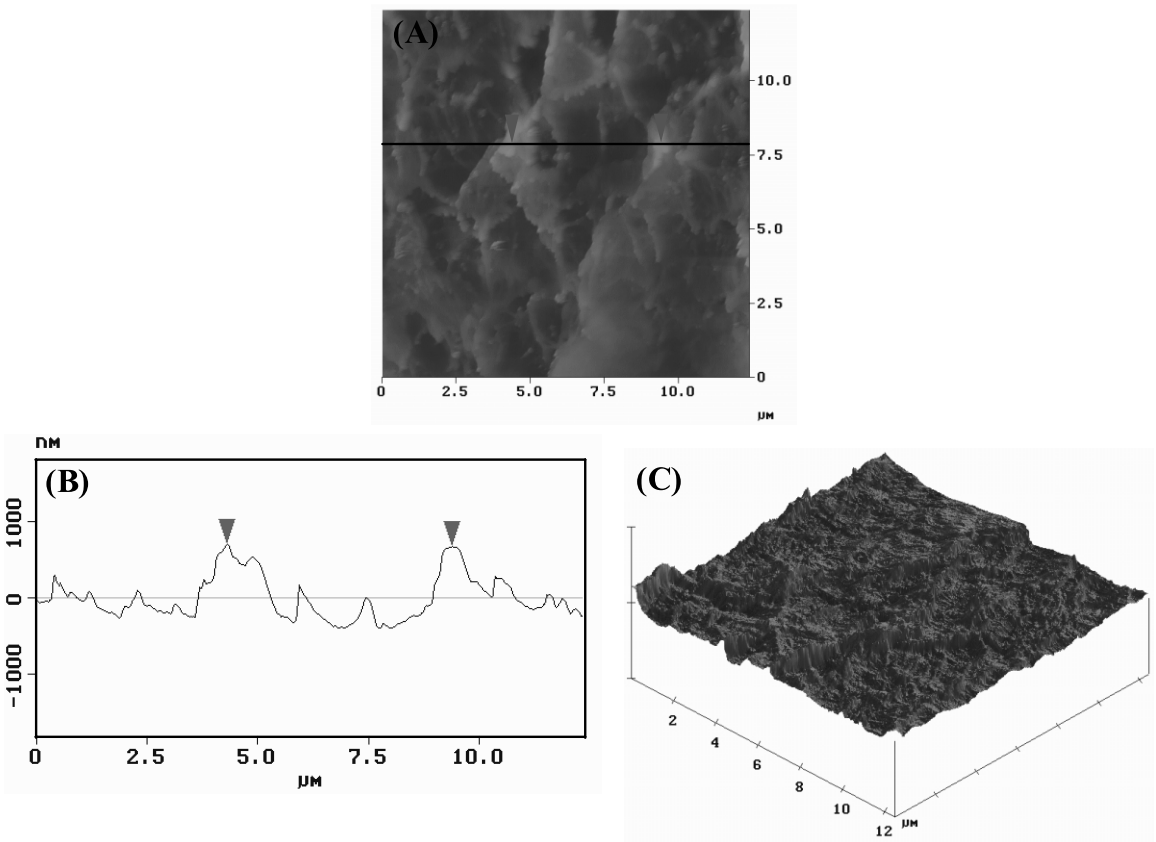

Fig. 4. (A) AFM image, (B) sectional view along the line in the AFM image, and (C) three-dimensional topography for pure iPS.

($\delta \sim 18.6$ MPa$^{1/2}$) [56], which is a better solvent for the iPS segment.

Fig. 6 shows (A) AFM image and (B) sectional view along the line in the AFM image for iPS/P4MS = 10/90. It marks an area of 12.4 μm × 12.4 μm, which represents the area in which the data analysis was performed. Therefore, many fine drops of the protruding structure and roughness are detected, which is similar the surface structure of pure P4MS. Note that the black and white contrast represent relative heights and thus the drops mostly appear in black.

As the polymer composition was changed to iPS/P4MS = 50/50, the surface of the blend tended to show a completely immiscible structure. Fig. 7 shows the AFM topography of iPS/P4MS = 50/50 sample, which is a two-phase structure typified with white and black regions. The surface shows the protruding topography, which is similar to the surface structure of neat iPS. The continuous surface has a height of about 1000 nm higher than the isolated islands. When the sample composition was changed to iPS/P4MS = 70/30, the isolated islands became even smaller. Fig. 8 shows the AFM image and sectional view for iPS/P4MS = 70/30. Since the apparent area of the brighter part in the AFM image increases with the weight fraction of iPS, it seems reasonable to conclude that the higher height region at the phase-separation surface is composed of the iPS-rich phase, which has higher solubility in THF comprising with P4MS. This indicates that the iPS continuous domains are composed of the iPS-rich phase. As discussed in the previous section, the amount of P4MS dissolved in the iPS-rich phase is greater than the amount of iPS dissolved in the P4MS-rich phase.

Kajiyama et al. [24,25,31] have schemed the formation process of the surface phase-separated structure during evaporation of solvent for several immiscible binary blend systems. This concept can be extended to the present blend of iPS/P4MS, which can be similarly described in Fig. 9(A)–(C). An as-blended iPS/P4MS solution before drying is depicted as shown in Fig. 9(A). Since the time required for the surface formation is fairly short due to fast evaporation of the solvent, a surface containing both iPS and P4MS components with some residual solvent is formed, as shown in Fig. 9(B). Then, the iPS-rich phase finally separates out of the film surface, as shown in Fig. 9(C). The formation process of the surface phase-separated structure can be explored as follows. P4MS segments with a lower free surface energy tend to cover the air-polymer interfacial region in order to minimize the interfacial free energy. Then, the P4MS-rich phase is preferably spread out over the surface. Therefore, if the total area of the film remains constant, the iPS-rich phase protrudes from the film surface. Two distinct types of fracture surface morphologies and corresponding phase relationships are observed in the iPS/P4MS blend system, and these two types are: (1) a single phase which is similar the morphology feature of pure

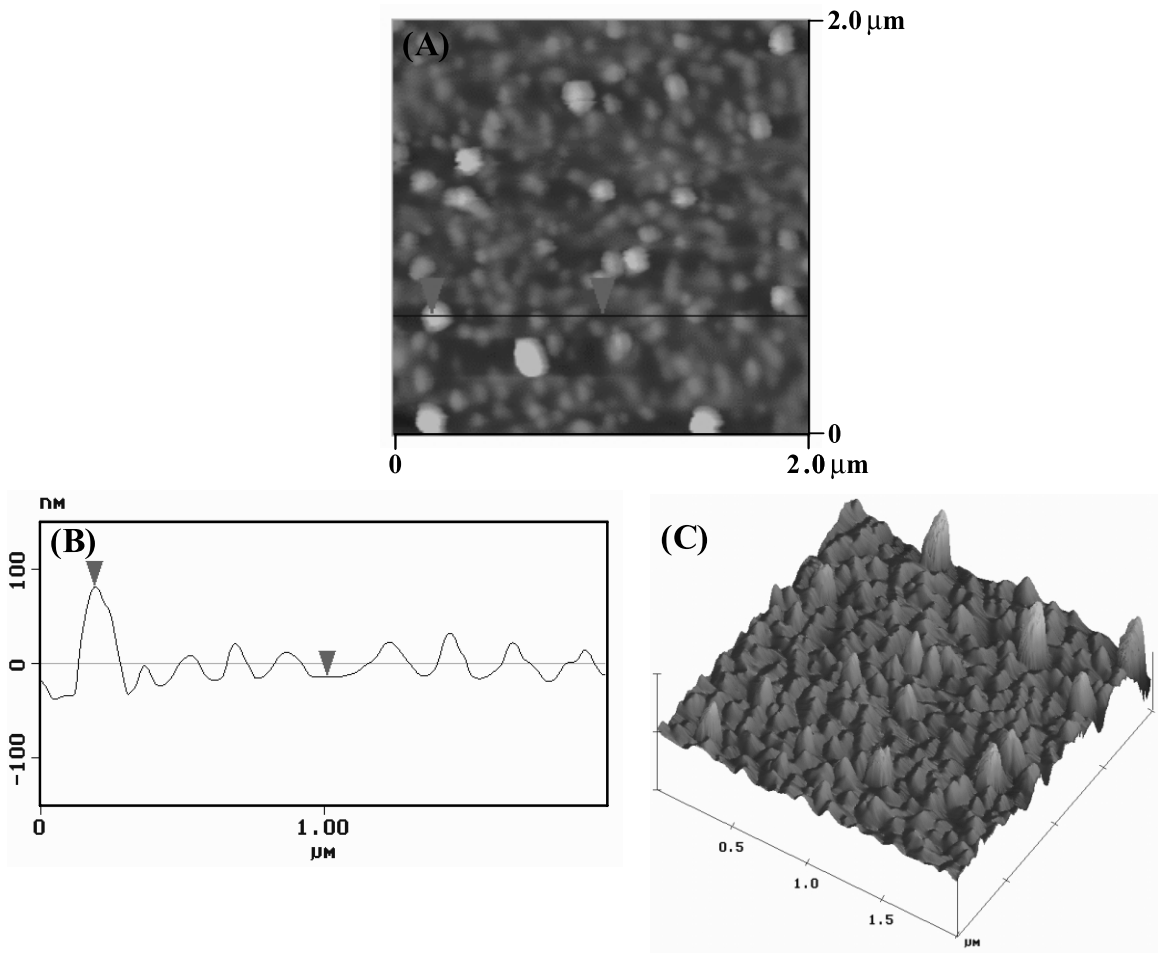

Fig. 5. (A) AFM image, (B) sectional view along the line in the AFM image, and (C) three-dimensional topography for pure P4MS.

P4MS; and (2) separated phases in which P4MS is the dispersed phase and iPS is the continuous phase.

4. Conclusion

From the result of the T_g's and phase composition of iPS/P4MS blends, it can be concluded that the apparent weight fraction of the P4MS component dissolves in the iPS-rich phase than does iPS in the P4MS-rich phase, which is consistent with the behavior of the ΔC_p of iPS in the iPS/P4MS blend system. This study attempted to compare the values of χ_{12} obtained by two different methods based on: (1) the glass transition temperatures of separated phases, and (2) the UCST data. These two methods have been shown to be in good agreement for the χ_{12} values as demonstrated in the model system of iPS/P4MS blend that shows a UCST behavior and separated phases below the UCST temperatures. It is interesting to note that the χ_{12} increases with the increasing weight fraction of iPS and indicates that the compatibility increases more in the region of P4MS-rich compositions than in the region of iPS-rich compositions in blends of iPS/P4MS. The AFM result shows that the phase-separated structure is more pronounced in the blend system containing higher iPS contents (e.g. iPS wt fractions = 0.7 and 0.5 in blends) than those with lower iPS contents (e.g. iPS wt fraction = 0.1 or smaller). This AFM observation is consistent with the conclusion of T_g result.

Two distinct types of fracture surface morphologies and corresponding phase relationships are observed in the iPS/P4MS blend system, and these two types are: (1) a single phase which is similar the morphology feature of pure P4MS; and (2) separated phases in which P4MS is the dispersed phase and iPS is the continuous phase. The morphology reveals that P4MS is the main constituent material for the dispersed phase and iPS is for the continuous phase. Another important aspect of surface morphology is that iPS excludes from the surface while P4MS enriches on the surface. The formation of the blend morphology seems to be governed by two factors. One is that the solubilities of these two polymers in the solvent tend to be different. The other is that P4MS has a marginally lower surface free energy than iPS ($\gamma = 40.7$ and 38.7 mJ/m^2 for iPS and P4MS, respectively). The surface morphology and trend of variation in the phase-separated

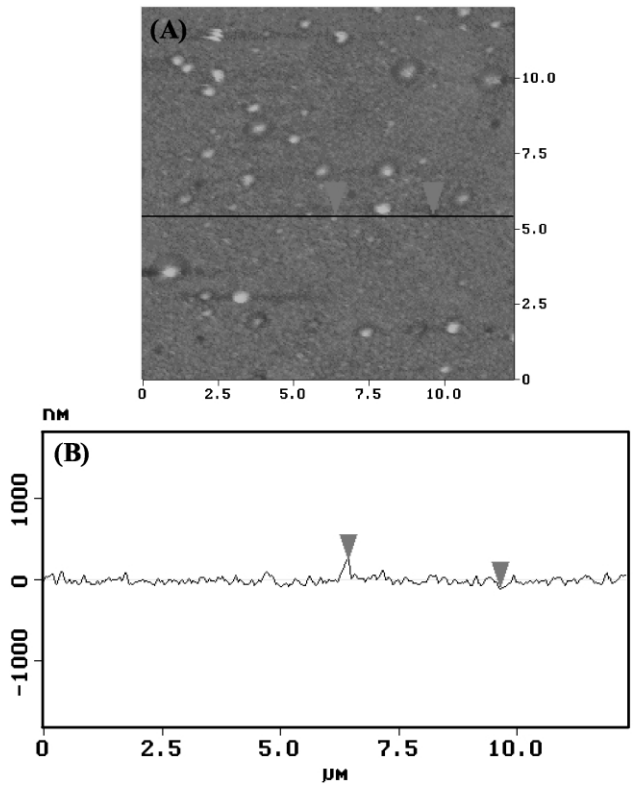

Fig. 6. (A) AFM image and (B) sectional view along the line in the AFM image for iPS/P4MS = 10/90.

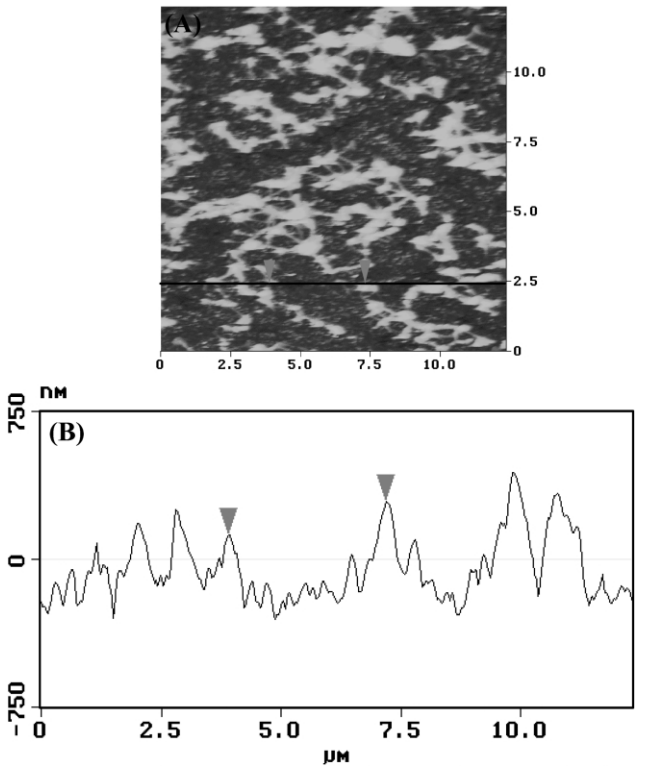

Fig. 8. (A) AFM image and (B) sectional view along the line in the AFM image for iPS/P4MS = 70/30.

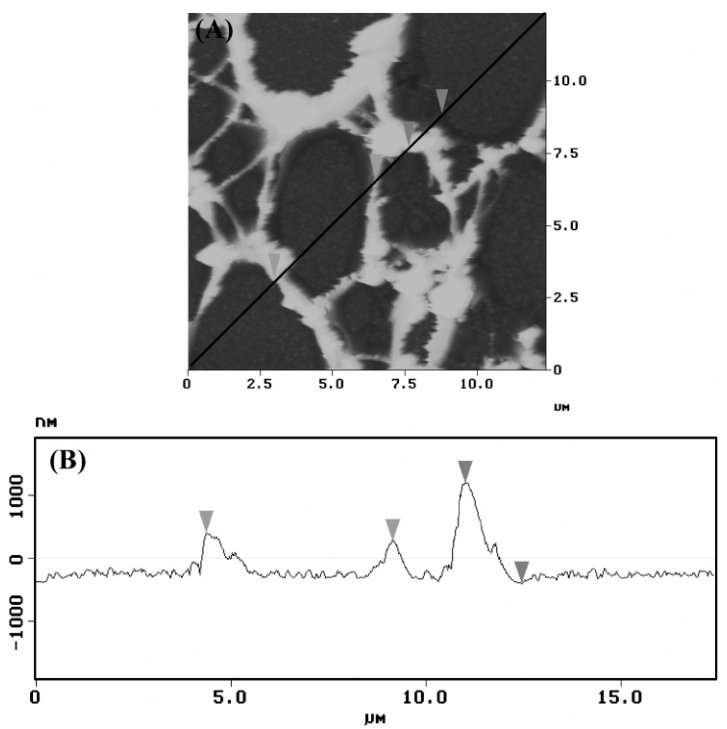

Fig. 7. (A) AFM image and (B) sectional view along the line in the AFM image for iPS/P4MS = 50/50.

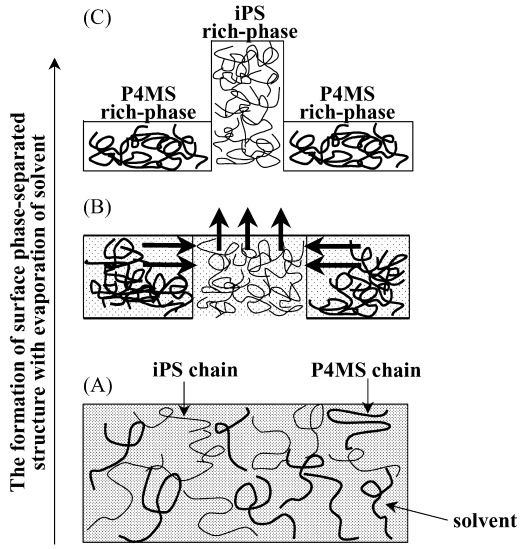

Fig. 9. Schematic representation of the formation process of the surface phase-separated structure of iPS/P4MS. (A) the bottom diagram shows iPS and P4MS segments in the solution, (B) the center diagram corresponds to formation of the phase-separated structure on the way, and (C) the top diagram shows a completed phase-separated morphology [25,28,54].

mechanism for the iPS/P4MS blend system with respect to the surface free energy and solubility in solvent is similar to many blend systems of PS/PMMA [25–28,55], PC/PMMA [57,58], PEO/PMMA [59], and PEA/PS [60], suggesting that the surface free energy and solubility do influence the surface morphology of the immiscible blend systems.

Acknowledgements

This study is sponsored by fundamental research grants provided by Taiwan's National Science Council (#NSC90-2216-006-030).

References

[1] Woo EM, Jang FH. Polymer 1999;40:2803.
[2] Callaghan TA, Paul DR. Macromolecules 1993;26:2439.
[3] Stroeks A, Paquaij R, Nies E. Polymer 1991;32:2653.
[4] Londono JD, Wignall GD. Macromolecules 1997;30:3821.
[5] Lang S, Sillescu H. Makromol Chem 1989;190:797.
[6] Chang LL, Woo EM. Macromol Chem Phys 2001;202:636.
[7] Chang LL, Woo EM. Colloid Polym Sci 2002; revised.
[8] Roe RJ, Zin WC. Macromolecules 1980;13:1221.
[9] Paul DR, Newman S, editors. Polymer Blends, vols. 1 and 2. New York: Academic Press; 1978.
[10] Robard A, Patterson D. Macromolecules 1977;10:1021.
[11] McMaster LP. Macromolecules 1973;6:760.
[12] Liu DD, Prausnitz JM. Macromolecules 1979;454.
[13] Patterson D. Macromolecules 1969;2:672.
[14] Patterson D. J Polym Sci, Part C 1968;16:3379.
[15] Scholte ThG. J Polym Sci, Part A-2 1971;9:1533.
[16] Derham KW, Goldsbrough J, Gordon M. Pure Appl Chem 1974;38:97.
[17] Berek D, Lath D, Durdovic V. J Polym Sci, Part C 1967;C16:659.
[18] Shultz AR, McCullough CR. J Polym Sci, Part A-2 1972;10:307.
[19] Kim WN, Burns CM. J Appl Polym Sci 1987;34:945.
[20] Kim WN, Burns CM. Macromolecules 1987;20:1876.
[21] Kim WN, Burns CM. Polym Engng Sci 1988;28:1362.
[22] Kim WN, Burns CM. J Polym Sci, Polym Phys Ed 1990;28:1409.
[23] Ton-That C, Shard AG, Daley R, Bradley RH. Polymer 2001;42:1121.
[24] Kajiyama T, Takahara A, Tanaka K. Macromolecules 1996;29:3232.
[25] Kajiyama T, Takahara A, Tanaka K. Macromolecules 1995;28:934.
[26] Chiou JS, Barlow JW, Paul DR. J Polm Sci, Part B 1987;25:1459.
[27] Lhoest JB, Bertrand P, Weng LT, Dewez JL. Macromolecules 1995;28:4631.
[28] Parent RR, Thompson EV. J Polym Sci, Polym Phys Ed 1978;16:1829.
[29] Davies MC, Shakesheff KM, Shard AG, Domb A, Roberts CJ, Tendler SJB, Williams PM. Macromolecules 1996;29:2205.
[30] Ton-That CA, Shard G, Daley R, Bradley RH. Macromolecules 2000;33:8453.
[31] Takahara A, Nakamura K, Tanaka K, Kajiyama T. Macromol Symp 2000;159:89.
[32] Durigon PER, Petri DFS, Drings H, Schimmel Th, Bruns M. Colloid Polym Sci 2001;279:1013.
[33] Krausch G, Hipp M, Boltau M, Matri O, Mlynek J. Macromolecules 1995;28:260.
[34] Jackson ST, Short RD. J Mater Chem 1992;2:259.
[35] Jones RAL, Kramer EJ, Rafailovich MH, Sokolov J, Schwarz SA. Phys Rev Lett 1989;62:280.
[36] Liu S, Chan CM, Weng LT, Jiang M. Macromolecules 2002;35:5623.
[37] Duan Y, Pearce EM, Kwei TK, Hu X, Rafailovich M, Sokolov J, Zhou K, Schwarz S. Macromolecules 2001;34:6761.
[38] Kim WN, Burns CM. J Appl Polym Sci 1990;41:1575.
[39] Lee HS, Kim WN, Burns CM. J Appl Polym Sci 1997;64:1301.
[40] Chun YS, Lee HS, Kim WN. Polym Engng Sci 1996;36:2694.
[41] Chun YS, Lee HS, Yoon HG, Kim WN. J Appl Polym Sci 2000;78:2488.
[42] Wood LA. J Polym Sci 1958;28:319.
[43] Stoelting J, Karasz FE, MacKnight WJ. Polym Engng Sci 1970;10:133.
[44] Fox TG. Bull Am Phys Soc 1956;1:123.
[45] Couchman PR. Macromolecules 1978;11:1156.
[46] Couchman PR, Karasz FE. Macromolecules 1978;11:117.
[47] Fried JR, Karasz FE, MacKnight WJ. Macromolecules 1978;11:150.
[48] Brinke G, Karasz FE, Ellis TS. Macromolecules 1983;16:244.
[49] Shultz AR, Young AL. J Appl Polym Sci 1983;16:1677.
[50] Krause S, Iskandar M, Iqbal M. Macromolecules 1982;19:55.
[51] Flory PJ. Principles of polymer chemistry. Ithaca/London: Cornell U. Press; 1978. Chapter 12.
[52] Roe RJ. Adv Chem Ser 1979;176:599.
[53] Tompa H. Trans Faraday Soc 1949;45:1142.
[54] Scott RL. J Chem Phys 1949;17:279.
[55] Karam HJ, Polymer compatibility and incompatibility, vol. 2. Switzerland: MMI Press Symposium Series; 1982. p. 93.
[56] Brandrup J, Immergut EH, Grulke EA. Polymer handbook. New York: Wiely; 1999.
[57] Viville P, Biscarini F, Bredas JL, Lazzaroni R. J Phys Chem B 2001;105:7499.
[58] Lhoest J-B, Bertrand P, Weng LT, Dewez J-L. Macromolecules 1995;28:4631.
[59] Ferreiro V, Douglas JF, Amis EJ, Karim A. Macromol Symp 2001;167:73.
[60] Raghavan D, Gu X, VanLandingham M, Nguyen T. Macromol Symp 2001;166:297.